Available online at www.sciencedirect.com
SCIENCE DIRECT®
Journal of Magnetic Resonance 168 (2004) 346–351
JMR Journal of Magnetic Resonance
www.elsevier.com/locate/jmr

Communication

Enhancing MQMAS sensitivity using signals from multiple coherence transfer pathways

Zhehong Gan* and Hyung-Tae Kwak

National High Magnetic Field Laboratory, Center of Interdisciplinary Magnetic Resonance, Tallahassee, FL 32310, USA

Received 4 February 2004; revised 20 March 2004
Available online 21 April 2004

Abstract

Multiple-quantum magic-angle spinning experiment removes second-order quadrupolar broadening from the central-transition of half-integer quadrupolar nuclei. This paper presents a novel scheme to enhance the sensitivity of MQMAS using signals from multiple coherence transfer pathways. The enhancement can be obtained in two ways. The first method uses the multiplex phase cycling to acquire MQMAS spectra from various coherence transfer pathways simultaneously. An addition of spectra collected with no extra time enhances the efficiency of the experiment. The second method, soft-pulse-added-mixing, is designed based on a complete alias of coherence transfer pathways. By properly fixing the soft-pulse phase, signals from various coherence transfer pathways can add constructively resulting higher signal intensities. The two methods are demonstrated for sensitivity enhancement with samples of spin—3/2 and 5/2.

1. Introduction

Multiple-quantum magic-angle-spinning (MQMAS) experiment introduced by Frydman and Harwood [1] has become the method of choice for obtaining high-resolution solid-state NMR spectra of quadrupolar nuclei with half-integer spins. The experiment correlates multiple-quantum and single-quantum central-transitions under magic-angle-spinning yielding ridge-shaped peaks in the 2D spectra. A shearing transformation can lead to high-resolution isotropic NMR spectra along one of the two dimensions.

Since the discovery of MQMAS, the development of the experiment has been mainly in two areas. First, numerous pulse schemes have been designed to improve the efficiencies of multiple-quantum excitation and conversion [2–17]. Second, several acquisition methods were introduced for obtaining 2D MQMAS spectra with absorptive lineshape. In the original MQMAS experiment, a single mixing-pulse was used for the MQ → CT coherence transfer. The signal from the echo coherence transfer pathway is *phase-modulated* with respect to t_1 and a 2D Fourier transformation gives rise to phase-twisted spectral lineshape [2]. The more desirable absorptive lineshape can be obtained with both the *echo* and the *anti-echo* signals. By adding a so-called *z-filter*, the two signals can be acquired with equal amplitude resulting in *amplitude-modulated* signals with respect to t_1. A hypercomplex Fourier transformation gives rise to pure absorptive spectral lineshape [18]. Absorptive lineshape can also be obtained with signals from just one coherence transfer pathway. The spectral lineshape of the phase-modulated data becomes absorptive if the signals are shifted in the time-domain by a spin-echo and *whole-echoes* are acquired for all t_1-increments. The *shifted-echo* scheme was originally introduced for the dynamic-angle spinning (DAS) experiment [19] and was incorporated with the MQMAS experiment [20]. The *shifted-echo* experiment can also be modified to a *split-*t_1 version. By programming the t_2-acqusition window following the *echo* or *anti-echo* signals, isotropic spectra can be obtained directly without the need of shearing transformation [21]. It should be noted that the *echo*-type MQMAS experiments require relatively long spin-echo delays for *whole-echo* acquisition and signal intensities are subject to the homogeneous part of T_2 relaxation. For this reason, the *echo*-type experiments

* Corresponding author. Fax: 1-850-644-1366.
E-mail address: gan@magnet.fsu.edu (Z. Gan).

1090-7807/$ - see front matter © 2004 Elsevier Inc. All rights reserved.
doi:10.1016/j.jmr.2004.03.021

are usually used for samples with large second-order quadrupolar shift and long T_2 relaxation.

The *z-filtered* and *echo* types of MQMAS experiment acquire signals from only one or a pair of symmetrical coherence transfer pathways. Signals from other pathways are averaged out during the phase cycling that selects the desired coherence transfer pathway [22]. In this communication, we propose two methods that use signals from more coherence transfer pathways to enhance MQMAS sensitivity. The first method uses recently introduced multiplex version of phase cycling [23]. Multiplex phase cycling stores signals individually when incrementing pulse phase. Coherence transfer pathway selections are performed only after data acquisition by summing stored signals multiplied with a phase factor similar to the receiver phase in the conventional phase cycling. Thus, signals from all coherence transfer pathways can be obtained from one complete cycle acquired in the multiplex manner. By adding MQMAS spectra from many coherence transfer pathways collected with no extra time, the signal-to-noise ratio can be enhanced over the conventional phase cycling that selects signals from only one or a pair of coherence transfer pathways.

The second method uses a complete alias of coherence transfer pathway. By fixing the pulse phase and skipping its cycling, signals from all coherence transfer pathways are aliased. It will be shown that for MQMAS experiment with a central-transition selective pulse signals from three coherence transfer pathways can be added constructively leading to an efficient mixing scheme we call soft-pulse-added-mixing (SPAM). In the following, we first describe the picture of various coherence transfer pathways for the MQMAS experiment. We then present the multiplex phase cycling and SPAM methods that use signals from multiple coherence transfer pathways for sensitivity enhancement.

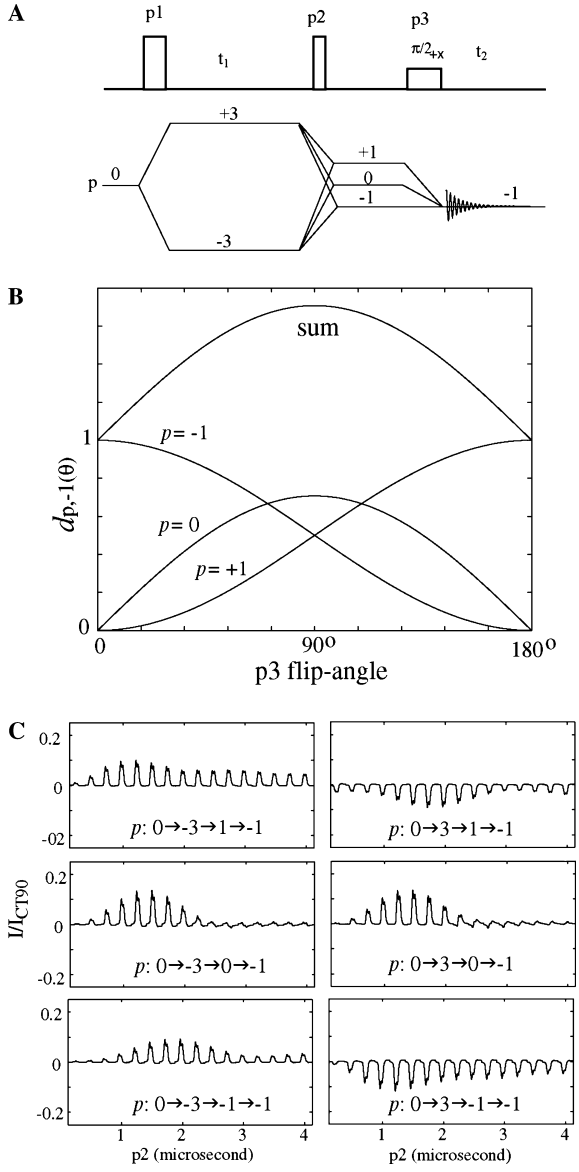

Fig. 1. (A) Three-pulse MQMAS sequence and coherence transfer pathways, (B) theoretical soft-pulse mixing curves, and (C) experimental strong-pulse mixing curves with arrays of $^{27}AlPO_4$-berlinite spectra. All measurements were performed at 19.6 T (216.13 MHz for ^{27}Al) with a Bruker DRX console and a home-built 4 mm MAS probe. The rf field was at $\gamma B_1/2\pi = 90$ kHz during the first ($p1 = 4\,\mu s$) and the second pulses and lowered to 9.3 kHz during the 90° soft-pulse ($p3 = 9\,\mu s$). The spectral intensities were measured with a few microseconds delays among the three pulses and normalized with a 1D spectrum acquired by a central-transition selective 90° pulse with the same 5 s recycle delay and 5 kHz spinning frequency.

2. Multiple coherence transfer pathways

Both the *z-filtered* and *echo*-type MQMAS experiments use two mixing pulses to convert coherence from the multiple-quantum transition ($p = \pm 3$) to the single-quantum central-transitions for detection ($p = -1$). The first mixing pulse usually employs a strong rf field for $MQ \rightarrow CT$ conversion. The second mixing pulse was introduced for balancing between the *echo* and *anti-echo* amplitudes in the case of the *z-filtered* experiment and for *whole-echo* acquisition in the case of *echo*-type experiments. It uses a much weaker rf field to confine the mixing of the three $p = 0, \pm 1$ coherences within the two-level central-transition system. The two-step transfer leads to three possible coherence transfer pathways each for the *echo* and *anti-echo* signals (Fig. 1A). In the past, most of the efforts have been concentrated on optimizing the first conversion pulse using strong and modulated rf fields. Here we focus on the role of the soft mixing pulse and optimal use of signals from all three coherence transfer pathways (we label the three pathways as $p = 0, \pm 1$ for the remaining of the paper).

The signal intensity is proportional to the product of the two-step mixing efficiencies. For the soft-pulse, coherence transfer within the two-level central-transition

system can be described by reduced Wigner rotation matrix elements

$$d^1_{p,-1}(\theta) = \left(\frac{1-\cos\theta}{2}, \frac{-\sin\theta}{\sqrt{2}}, \frac{1+\cos\theta}{2}\right),\ p = +1, 0, -1. \tag{1}$$

$\theta = (S+1/2)\gamma B_1 p_3$ is the pulse flip-angle by the weak rf field selective to the two-level central-transition system of the half-integer spin. Fig. 1B plots the coherence transfer as a function of θ. For a 90° pulse $d^1_{p,-1}(\pi/2) = (1/2, -\sqrt{2}/2, 1/2)$, the soft-pulse reduces the signal intensity by 70% for the $p = 0$ pathway and by 50% for the $p = \pm 1$ pathways. For the strong mixing pulse, the spin dynamics of a multi-level system is more complicated and an analytical expression for the coherence transfer is difficult to obtain. Fig. 1C shows the strong-pulse mixing curves measured experimentally using a model compound. These mixing curves were measured with an optimized MQ excitation, a 90° soft-pulse and very short delays among the three pulses. Time evolution of multiple-quantum and central-transition coherences during these short delays can be neglected. The signal phase comes solely from the multiplication of multi-step coherence transfers. Considering the scaling by $d^1_{p,-1}(\pi/2) = (1/2, -\sqrt{2}/2, 1/2)$, one can see that the mixings by the strong pulse via the three coherence transfer pathways have similar peak amplitudes. The mixings reach their peak intensities at pulse length in the order of $p2_{\Delta p=2} < p2_{\Delta p=3} < p2_{\Delta p=4}$.

Considering the signal from only one coherence transfer pathway, adding the second mixing pulse always reduces the overall efficiency. The soft pulse is though needed for absorptive lineshape by balancing between *echo* and *anti-echo* amplitudes or *whole-echo* acquisition. However, if one includes signals from three coherence transfer pathways, it is possible to gain sensitivity with the addition of the soft-pulse. Fig. 1B shows the sum of three mixing curves. The total signal intensity increases with the soft-pulse flip-angle and reaches the maximum at $1+\sqrt{2}/2$ with $\theta = 90°$, indicating the possibility of a 70% increase assuming identical mixing from the $3Q$ coherence by the strong mixing pulse. The next two sections will describe how the multiplex phase cycling and the SPAM methods are designed using signals from all three coherence transfer pathways for sensitivity enhancement.

3. Multiplex phase cycling

The mixing curves in Fig. 1C show comparable signal intensities from the three coherence transfer pathways with a 90° soft mixing pulse. The *z*-filtered MQMAS experiment uses the signals from the $p: 0 \to \pm 3 \to 0 \to -1$ pathways. During the conventional phase cycling for coherence transfer pathway selection, signals from other pathways are averaged out and lost irreversibly. Recently Ivchenko et al. [23] introduced a multiplex version of phase cycling that can avoid this kind of signal loss. The multiplex method was originally designed for reducing phase cycling steps. It stores signals individually when incrementing pulse phase, and signal average occurs only after data acquisition. We use this phase cycling here to simultaneously acquire signals from multiple coherence transfer pathways for sensitivity enhancement.

We describe here an explicit two-step version of multiplex phase cycling for the MQMAS experiment. A general description about multiplex phase cycling can be found in [23]. For the pulse sequence in Fig. 1A, the excitation pulse and the receiver phase are cycled in 6×2 steps in the conventional manner that selects the $\pm 3Q$ signals in the hyper-complex format. The soft-pulse is phase cycled between $+x$ and $-x$ in a two-step multiplex manner and the strong mixing pulse is fixed at $+x$. Four signals $C_{+x}, S_{+x}, C_{-x}, S_{-x}$ are stored in a complete phase cycle of 24 scans for each t_1-increment. After the completion of data acquisition, one can construct two hypercomplex data sets

$$\begin{aligned} C_0 &= C_{+x} + C_{-x}, \quad S_0 = S_{+x} + S_{-x}, \\ C_1 &= C_{+x} - C_{-x}, \quad S_1 = S_{+x} - S_{-x}. \end{aligned} \tag{2}$$

C_0, S_0 are simply the signals of the *z-filtered* experiment. C_1, S_1 are the aliased signals from the $p = \pm 1$ pathways. It should be noted that the two spectra are acquired at the same time rate as the *z-filtered* experiment. The only cost for the multiplex phase cycling is doubling the data storage.

This two-step multiplex phase cycle is designed based on the mixing curves in Fig. 1C. Assuming an ideal central-transition selective pulse, a two-step phase cycle is sufficient to select the $p = 0$ pathway because coherence transfer via $|p| > 1$ orders can be neglected. The two-step cycle cannot separate the two $p = \pm 1$ pathways. However, Fig. 1C shows that $p = \pm 1$ mixing curves have the same signs for both the *echo* and *anti-echo* pathways. Therefore, a two-step phase cycle aliases the two pathways adding up their signals constructively. The sum of the two $p = \pm 1$ mixing curves in Fig. 1C is higher than the $p = 0$ z-filtered one. Furthermore, the two-step multiplex phase cycle acquires the ($p = 0$ and the $p = \pm 1$) MQMAS spectra simultaneously. The two spectra can be added together, optimally weighted by their peak intensities for additional sensitivity enhancement. The signal-to-noise (S/N) ratios among the summed, the $p = \pm 1$ aliased and the *z-filtered* spectra are $\sqrt{(I_{+1}+I_{-1})^2/I_0^2 + 1} : |(I_{+1}+I_{-1})/I_0| : 1$, where $I_{0,\pm 1}$ are the signals from the three $p = 0, \pm 1$ pathways, respectively. Fig. 1C shows that with a 1.5 μs mixing pulse the signal intensities from the three coherence transfer pathways are approximately $I_{+1} = 0.09, I_0 = 0.13$,

$I_{-1} = 0.08$. Therefore, the S/N ratio is enhanced by about 64% with the two-step multiplex phase cycling over the *z-filter* experiment.

Pure absorptive spectra require equal amplitude between the *echo* and *anti-echo* signals. This requirement is fulfilled for the two *z-filtered* pathways as pulsed coherence transfer can always be described by a unitary transformation [24]. For the aliased $p = \pm 1$ spectra, this requirement is not automatically fulfilled. The imbalance between the *echo* and *anti-echo* signals can be derived as $(a_{\Delta p=2} - a_{\Delta p=4})\cos\theta$, where $a_{\Delta p=2,4}$ are the coherence transfer amplitudes by the strong mixing pulse. Therefore, a 90° soft-pulse yields balanced *echo* and *anti-echo* signals for the $p = \pm 1$ MQMAS spectra. This flip-angle also gives the maximal intensity for the z-filtered signals. As for the strong mixing pulse, the optimal pulse length is usually near the peak for the $p = 0$ mixing curve (Fig. 1C). At this pulse length, the $p = \pm 1$ curves show similar intensities, one slightly before ($|\Delta p| = 4$) and the other a little beyond ($|\Delta p| = 2$) their optimal pulse length. The close signal intensities help to reduce the difference between *echo* and *anti-echo* amplitudes $(a_{\Delta p=2} - a_{\Delta p=4})\cos\theta$ in the case of a mis-calibrated 90° soft-pulse.

3.1. Soft-pulse-added-mixing

The multiplex phase cycling method described above acquires both *echo* and *anti-echo* signals for pure absorptive MQMAS spectra. When considering only one of the two $\pm 3Q$ signals, we can extend the alias of coherence transfer pathways further to add signals from all three coherence transfer pathways. On the left side of Fig. 1C, the $p = 0, \pm 1$ mixing curves for the $p = -3$ pathways all have positive sign. Thus, fixing the soft-pulse phase to $+x$ aliases the three pathways adding the three signals together. For the $p = 3$ pathways on the right, the three curves show different signs. A switch of the soft-pulse phase to $-x$ reverses the sign for $p = 0$ curve ($\Delta p = -1$) while keeping the other two the same ($\Delta p = 0, -2$). Thus, the sign of all three curves become negative and a complete alias adds the signals together constructively. As we can consider the two pulses with fixed phase as one mixing element, we call it SPAM.

Fig. 2 shows the soft-pulse flip-angle dependence of the experimentally measured mixing curves demonstrating the enhanced efficiencies by SPAM. The curves for 90° soft-pulse are higher than the ones without the soft-pulse ($\theta = 0°$) for both $p : \pm 3 \rightarrow -1$ mixings. The enhancement is more than 50% for the $p : +3 \rightarrow -1$ mixing and is about 30% for the $p : -3 \rightarrow -1$ mixing. It can be seen that the two mixing curves with $\theta = 90°$ are nearly identical indicating equal amplitude between the *echo* and *anti-echo* signals. This is an experimental demonstration of balanced *echo* and *anti-echo* signals by a calibrated $\theta = 90°$ soft-pulse as discussed in the previous section for absorptive lineshape.

In *shifted-echo* or split-t_1 type of MQMAS experiment, an additional 180° soft-pulse is inserted before the signal detection and the coherence transfer pathways follow the $p : 0 \rightarrow \pm 3 \rightarrow +1 \rightarrow -1$. It should be noted that the $p : \pm 3 \rightarrow -1$ and $p : \mp 3 \rightarrow +1$ coherence transfers are complex conjugate to each other, therefore have the same amplitude. SPAM with a phase change

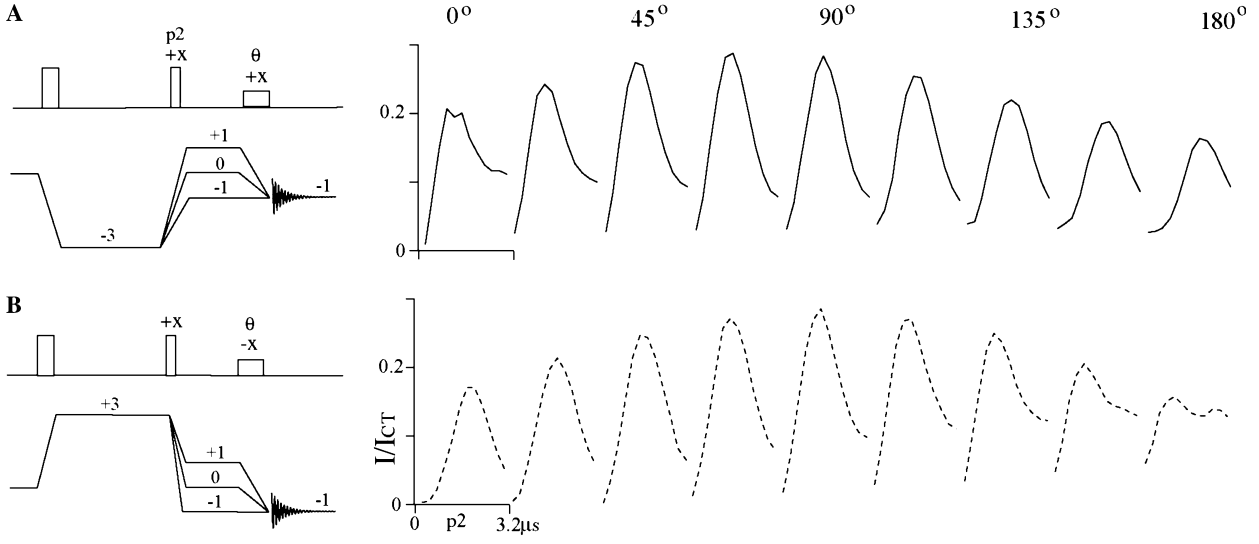

Fig. 2. Arrays of mixing curves demonstrating the enhancement by SPAM for (A) $p : -3 \rightarrow -1$ and (B) $p : +3 \rightarrow -1$ mixing. The mixing curves were measured from $^{23}Na_2SO_4$ peak intensity as a function of the strong mixing pulse length p2 and the soft-pulse flip-angle θ incrementing at 22.5° a step from 0 to 180°. The rf field was at $\gamma B_1/2\pi = 90$ kHz during the strong pulses and lowered to 9 kHz for the soft-pulse. The spectral intensities were measured with short delays (a few micro-seconds) among the three pulses and normalized with a 1D spectrum acquired with a central-transition selective 90° pulse under the same condition of 5 s recycle delay and 5 kHz spinning frequency. The signal enhancement comes from a complete alias of three coherence transfer pathways with fixed mixing pulse phase as shown on the left (note the soft-pulse phase change for the $p : +3 \rightarrow -1$ mixing).

enhances the $p: -3 \rightarrow +1$ mixing and one with the same phase should be used for the $p: +3 \rightarrow +1$ mixing. The incorporation of SPAM with numerous *echo*-type MQMAS experiments [21,25] can be easily implemented by considering the two mixing pulses as a single mixing element. In this short communication, we focus on the demonstration and the explanation of the sensitivity enhancement by the two methods based on using multiple coherence transfer pathways. Detailed results of SPAM with various MQMAS pulse sequences will be presented elsewhere and not discussed further here.

4. Conclusions

It has been shown that the efficiency of MQMAS experiment can be enhanced by using signals from multiple coherence transfer pathways. Two methods have been demonstrated for the sensitivity enhancement. The multiplex phase cycling method acquires signals from multiple coherence transfer pathways simultaneously. An addition of spectra collected with no extra time enhances the efficiency of the experiment. The SPAM method enhances the mixing efficiency by simply adding a soft-pulse with properly fixed phase after the strong mixing pulse. A soft-pulse without phase change enhances the $|\Delta p| = 2$ mixing and the one with a phase reverse enhances the $|\Delta p| = 4$ mixing. On the choice between the two methods, the multiplex phase cycling method is an extension to the *z-filtered* MQMAS experiment that acquires both *echo* and *anti-echo* signals for absorptive MQMAS spectra. The SPAM method enhances only one of the two $\pm 3Q$ signals and is usually combined with *shifted-echo* or *split-*t_1 type pulse sequences for absorptive MQMAS spectra. The relative efficiencies between the two methods depend on the T_2 and anisotropic second-order quadrupolar broadening of the sample. On the experimental aspect, the multiplex phase cycling requires additional data storage and a modification of processing software whereas the SPAM is simply an enhanced mixing element that requires no additional changes.

Using signals from multiple coherence transfer pathways for sensitivity enhancement may be generally extended to other NMR experiments such as MQMAS with modulated excitation and mixing elements, and STMAS [26] etc. The amount of gain depends whether coherence transfer pathways filtered out by conventional phase cycling have usable signals with comparable intensities.

Acknowledgments

This work is supported by the National High Magnetic Field Laboratory through National Science Foundation Cooperative Agreement DMR0084173 and by the State of Florida. The authors thank Professor Jean-Paul Amoureux (Lille, France) for discussions.

References

[1] L. Frydman, J.S. Harwood, Isotropic spectra of half-integer quadrupolar spins from bidimensional magic-angle-spinning NMR, J. Am. Chem. Soc. 117 (1995) 5367–5368.
[2] A. Medek, J.S. Harwood, L. Frydman, Multiple-quantum magic-angle spinning NMR: a new method for the study of quadrupolar nuclei in solids, J. Am. Chem. Soc. 117 (1995) 12779–12787.
[3] J.P. Amoureux, C. Fernandez, L. Frydman, Optimized multiple-quantum magic-angle spinning NMR experiments on half-integer quadrupoles, Chem. Phys. Lett. 259 (1996) 347–355.
[4] S.W. Ding, C.A. McDowell, Shaped pulse excitation in multi-quantum magic-angle spinning spectroscopy of half-integer quadrupole spin systems, Chem. Phys. Lett. 270 (1997) 81–86.
[5] G. Wu, D. Rovnyak, P.C. Huang, R.G. Griffin, High-resolution oxygen-17 NMR spectroscopy of solids by multiple-quantum magic-angle-spinning, Chem. Phys. Lett. 277 (1997) 79–83.
[6] J.P. Amoureux, C. Fernandez, Triple, quintuple and higher order multiple quantum MAS NMR of quadrupolar nuclei, Solid State Nucl. Mag. 10 (1998) 211–223.
[7] J.P. Amoureux, M. Pruski, D.P. Lang, C. Fernandez, The effect of RF power and spinning speed on MQMAS NMR, J. Magn. Reson. 131 (1998) 170–175.
[8] A.P.M. Kentgens, R. Verhagen, Advantages of double frequency sweeps in static, MAS and MQMAS NMR of spin $I = 3/2$ nuclei, Chem. Phys. Lett. 300 (1999) 435–443.
[9] F.H. Larsen, N.C. Nielsen, Effects of finite rf pulses and sample spinning speed in multiple-quantum magic-angle spinning (MQ-MAS) and multiple-quantum quadrupolar Carr-Purcell-Meiboom-Gill magic-angle spinning (MQ-QCPMG-MAS) nuclear magnetic resonance of half-integer quadrupolar nuclei, J. Phys. Chem. A 103 (1999) 10825–10832.
[10] P.K. Madhu, A. Goldbourt, L. Frydman, S. Vega, Sensitivity enhancement of the MQMAS NMR experiment by fast amplitude modulation of the pulses, Chem. Phys. Lett. 307 (1999) 41–47.
[11] A. Goldbourt, P.K. Madhu, S. Vega, Enhanced conversion of triple to single-quantum coherence in the triple-quantum MAS NMR spectrosocopy of spin-5/2 nuclei, Chem. Phys. Lett. 320 (2000) 448–456.
[12] P.K. Madhu, A. Goldbourt, L. Frydman, S. Vega, Fast radio-frequency amplitude modulation in multiple-quantum magic-angle-spinning nuclear magnetic resonance: theory and experiments, J. Chem. Phys. 112 (2000) 2377–2391.
[13] M. Pruski, J.W. Wiench, J.P. Amoureux, On the conversion of triple- to single-quantum coherences in MQMAS NMR, J. Magn. Reson. 147 (2000) 286–295.
[14] T. Vosegaard, D. Massiot, P.J. Grandinetti, Sensitivity enhancements in MQ-MAS NMR of spin-5/2 nuclei using modulated rf mixing pulses, Chem. Phys. Lett. 326 (2000) 454–460.
[15] Z. Yao, H.T. Kwak, D. Sakellariou, L. Emsley, P.J. Grandinetti, Sensitivity enhancement of the central transition NMR signal of quadrupolar nuclei under magic-angle spinning, Chem. Phys. Lett. 327 (2000) 85–90.
[16] T. Vosegaard, P. Florian, D. Massiot, P.J. Grandinetti, Multiple quantum magic-angle spinning using rotary resonance excitation, J. Chem. Phys. 114 (2001) 4618–4624.
[17] Z.H. Gan, P. Grandinetti, Rotary resonance in multiple-quantum magic-angle spinning, Chem. Phys. Lett. 352 (2002) 252–261.
[18] J.P. Amoureux, C. Fernandez, S. Steuernagel, Z filtering in MQMAS NMR, J. Magn. Reson. Ser. A 123 (1996) 116–118.
[19] P.J. Grandinetti, J.H. Baltisberger, A. Llor, Y.K. Lee, U. Werner, M.A. Eastman, A. Pines, Pure-absorption-mode lineshapes and

sensitivity in 2-dimensional dynamic-angle spinning NMR, J. Magn. Reson. Ser. A 103 (1993) 72–81.
[20] D. Massiot, B. Touzo, D. Trumeau, J.P. Coutures, J. Virlet, P. Florian, P.J. Grandinetti, Two-dimensional magic-angle spinning isotropic reconstruction sequences for quadrupolar nuclei, Solid State Nucl. Mag. 6 (1996) 73–83.
[21] S.P. Brown, S. Wimperis, Two-dimensional multiple-quantum MAS NMR of quadrupolar nuclei: a comparison of methods, J. Magn. Reson. 128 (1997) 42–61.
[22] G. Bodenhausen, H. Kogler, R.R. Ernst, Selection of coherence-transfer pathways in NMR pulse experiments, J. Magn. Reson. 58 (1984) 370–388.
[23] N. Ivchenko, C.E. Hughes, M.H. Levitt, Multiplex phase cycling, J. Magn. Reson. 160 (2003) 52–58.
[24] R.R. Ernst, G. Bodenhausen, A. Wokaun, Principles of Nuclear Magnetic Resonance in One and Two Dimensions, Clarendon Press, Oxford, 1987.
[25] T. Vosegaard, P. Florian, P.J. Grandinetti, D. Massiot, Pure absorption-mode spectra using a modulated RF mixing period in MQMAS experiments, J. Magn. Reson. 143 (2000) 217–222.
[26] Z.H. Gan, Isotropic NMR spectra of half-integer quadrupolar nuclei using satellite transitions and magic-angle spinning, J. Am. Chem. Soc. 122 (2000) 3242–3243.